Computational Materials Science 50 (2011) 2488–2492

Contents lists available at ScienceDirect

Computational Materials Science

journal homepage: www.elsevier.com/locate/commatsci

Investigating the effects of grain boundary energy anisotropy and second-phase particles on grain growth using a phase-field model

M. Asle Zaeem *, H. El Kadiri, P.T. Wang, M.F. Horstemeyer

Center for Advanced Vehicular Systems, Mississippi State University, Starkville, MS 39759, USA

ARTICLE INFO

Article history:
Received 8 February 2011
Received in revised form 21 March 2011
Accepted 24 March 2011
Available online 19 April 2011

ABSTRACT

A phase-field model was used to investigate the simultaneous effects of grain boundary energy anisotropy and the presence of second-phase particles on grain growth in polycrystalline materials. The system of grains with anisotropic grain boundary energies was constructed by considering models of low and high misorientation angles between adjacent grains. Systems without particles reached a steady state grain growth rate, and this rate decreased by including the grain boundary energy anisotropy. In addition, the presence of particles significantly altered the microstructures during grain growth. This study showed that for systems including particles, the critical average grain size to stop grain growth depends not only on the volume fraction and size of particles, but also on the grain boundary energy anisotropy.

1. Introduction

Mechanical properties of metallic alloys, such as their strength, hardness, ductility, elastic modulus, and toughness, are determined and controlled primarily by their grain microstructures [1]. Because of the extensive use of metallic components in different industries [1,2], predicting and controlling the microstructure evolution during different materials processing are of the most important tasks in materials science and engineering.

One of the most common microstructural evolutions resulting from different materials processing is grain growth [3–10]. There have been several numerical studies in this area based on different computational approaches such as the sharp interface [11–18], Monte Carlo [19–21], cellular automata [22,23], and phase field methods [24–30]. Most of these models either consider a single phase for the polycrystalline material without considering the pining effect of second-phase particles, or do not include the effects of anisotropic grain boundary energy on the microstructural evolution during the grain growth. The presence of second-phase particles can mitigate or even freezes the grain growth process and results in different microstructural configuration usually with finer grain sizes that can be accountable for different materials properties [30,31]. Grain growth process in the presence of second-phase spherical and stationary particles was considered by the Zener theory [32] and has been studied using the phase-field model by Moelans et al. [33,34] and Chang et al. [35]. Long et al. [29] used a similar phase-field model to study the effects of pre-aging δ-Ni_2Si particles on grain growth during re-aging process in Cu–Ni–Si alloy. These models did not include the important effects of anisotropic grain boundary energy resulted from misorientation angles between neighboring grains, which could lead to substantially different microstructures [36,37].

In this paper, a phase-field – finite element model is used to simulate the microstructural evolutions during grain growth considering the simultaneous effects of anisotropic grain boundary energy and second-phase particles on the growth rate. For the numerical computations, a finite element model similar to that developed in [38–40] is utilized.

2. Phase-field model

In the phase-field theory, a polycrystalline microstructure can be described by many orientation field variables or non-conserved order parameters ($\eta_i(\mathbf{r},t)$, $i = 1, 2, \ldots, n$, where n is number of different orientations) [24]. These field variables are continuous functions in time (t) and space dimensions ($\mathbf{r}$) and represent different orientations for different grains (Fig. 1). The value of the field variables varies between 0 and 1; for example for grains having the qth orientation: $\eta_{i=q}(\mathbf{r},t) = 1$ and $\eta_{i\neq q}(\mathbf{r},t) = 0$ and this transition from 0 to 1 in the grain boundaries is smooth (Fig. 2). The total grain boundary energy of a microstructure is a function of these field variables and their gradients. The free energy of the grains system including stationary particles (or inert particles) is [33–35]:

$$F = \int_V \left[f(\eta_1, \eta_2, \ldots, \eta_n) + \sum_{i=1}^{n} \frac{\kappa_i}{2} (\nabla \eta_i)^2 \right] dV, \quad (1)$$

* Corresponding author. Tel.: +1 509 432 3308.
E-mail address: mohsen@cavs.msstate.edu (M. Asle Zaeem).

0927-0256/$ - see front matter © 2011 Elsevier B.V. All rights reserved.
doi:10.1016/j.commatsci.2011.03.031

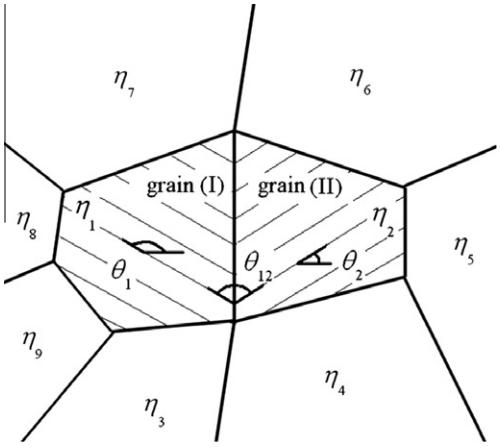

Fig. 1. Schematic of various crystal orientations using different orientation field variables for each grain. The solid-lines are grain boundaries.

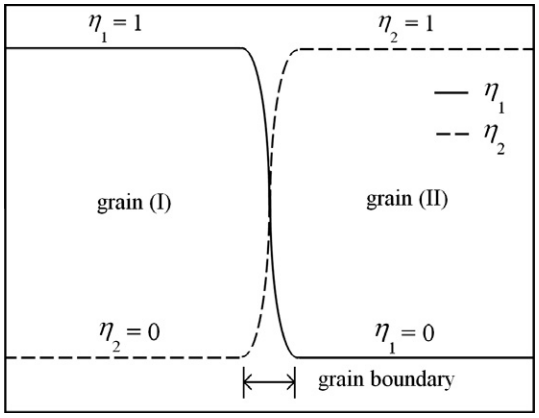

Fig. 2. Profiles of two field variables (η_1 and η_2) for the two neighboring grains in Fig. 1.

where κ_i are the gradient energy coefficients. The local free energy density, f, used by Moelans et al. [33,34], has this form:

$$f(\eta_1,\eta_2,\ldots,\eta_n)=\sum_{i=1}^{n}\left(-\frac{\alpha}{2}(\eta_i)^2+\frac{\beta}{4}(\eta_i)^4\right)+\gamma\sum_{i=1}^{n}\sum_{j\neq i}^{n}\eta_i^2\eta_j^2+\varepsilon\Phi^2\sum_{i=1}^{n}\eta_i^2, \tag{2}$$

α, β, γ, and ε are phenomenological parameters, and $\Phi = 1$ inside a particle and $\Phi = 0$ in the matrix. Here n is the number of different orientations for grains while no orientations are considered for particles. When $\Phi = 1$, f has one minimum at all η_i equal to 0. If in Eq. (2) ε is considered to be equal to γ, both Moelans et al. [33,34] and Chang et al. [35] models recover same results.

The evolution equations of non-conserved order parameters can be obtained from time-dependent Ginzburg–Landau (TDGL) [41] equation given by the following,

$$\frac{\partial\eta_i(\mathbf{r},t)}{\partial t}=-L_i\frac{\delta F}{\delta\eta_i(\mathbf{r},t)},\quad i=1,2,\ldots,n, \tag{3}$$

where L_i are the relaxation coefficients related to the grain boundary mobility.

To include misorientation angles between adjacent grains (angle θ_{ij} between grains i and j) which result in anisotropic grain boundary energies in the system, first we recall the relationship between gradient energy coefficient and grain boundary energy, $E(\theta_{ij})$, [37,42]:

$$\kappa_i=\overline{\kappa}_j E^2(\theta_{ij}),\quad \theta_{ij}=\theta_i-\theta_j, \tag{4}$$

where θ_i is the orientation angle of a grain with respect to a reference angle, and $\overline{\kappa}_j$ is considered to be a constant. Since in our model we are following the evolution of the order parameter and not the orientation angle of each grain, to calculate θ_{ij} for each grain boundary between two adjacent grains, we assume a random orientation angle ($\theta_i = [0 \quad \pi]$), which corresponds to each order parameter (Fig. 1).

A grain boundary energy model considering low misorientation angles between adjacent grains ($\theta_{ij} < 20°$) was presented by Read and Shockley (RS) [36]. In the RS model, the energy from low-angle grain boundaries was assumed to stem from two contributions: (1) energy from dislocation cores, E_c, and (2) energy from the strain field surrounding the dislocations, E_s:

$$E(\theta_{ij})=\theta_{ij}(E_c-E_s\ln|\theta_{ij}|). \tag{5}$$

The conventional form of Eq. (5) using a computational approach [27] is the following,

$$E(\theta_{ij})=E_0\frac{\theta_{ij}}{\theta_m}\left(1-\ln\left|\frac{\theta_{ij}}{\theta_m}\right|\right),\quad \theta_{ij}<\theta_m, \tag{6}$$

where E_0 is a material constant and is proportional to the total density of dislocations, and θ_m is the maximum misorientation angle for RS model ($\theta_m = 20°$). For $\theta_{ij} \geqslant 20°$, $E(\theta_{ij})/E_0 = 1$, same as isotropic cases (see Fig. 3). For large misorientation angles, modified RS (MRS), was developed by Wolf [43]:

$$E(\theta_{ij})=E_0\sin(2\theta_{ij})(1-r\ln|\sin(2\theta_{ij})|), \tag{7}$$

where r is a constant and in our simulations $r = 0.683$ same as [44] to make $(E(\theta_{ij})/E_0)_{max} = 1$.

In Fig. 3, the scaled grain boundary energy is plotted against the misorientation angles for the isotropic, RS, and MRS models.

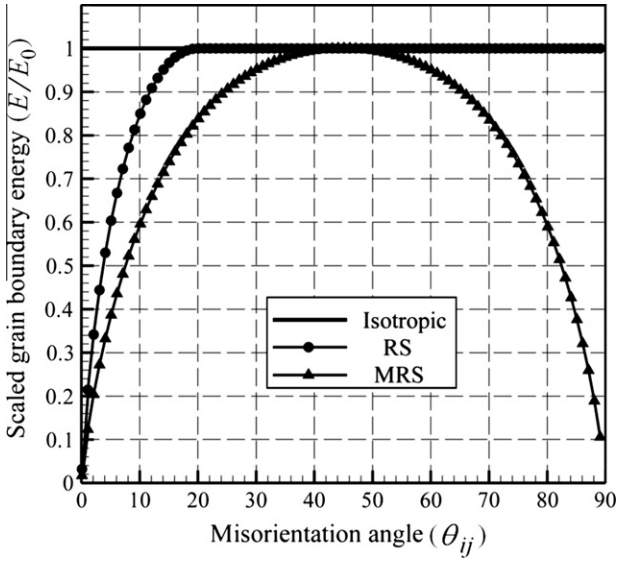

Fig. 3. Scaled grain boundary energy versus misorientation angle for the Read–Shockley (RS) model and the Modified Read–Shockley (MRS) model in comparison with the isotropic limiting case.

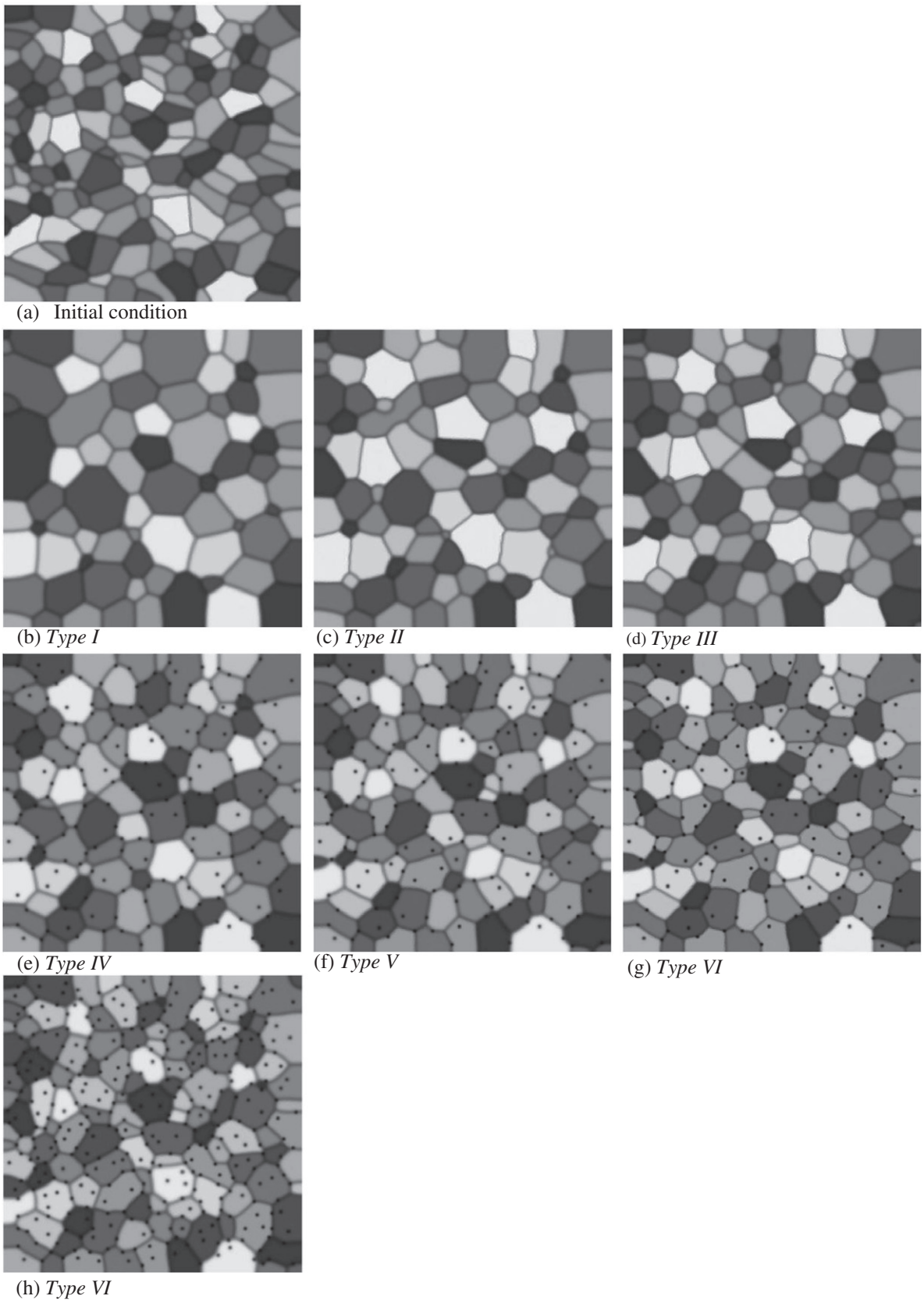

Fig. 4. Microstructural evolution. In (b–h) $t = 2000$. In (e–g) $V_f = 0.015$, and in (h) $V_f = 0.03$; $r_p = 2$ in (e–h).

3. Results and discussions

The parameters of the model are considered here to be constants, which closely correlates to the hypothesis to the original model by Fan and Chen [24]: $\alpha = \beta = \gamma = 1$ ($\varepsilon = \gamma$), $\overline{\kappa}_j = 2$, $L_i = 1$, and $E_0 = 1$ so that when $\theta_{ij} = \pi/4$ the value of the gradient energy coefficient becomes the same as an isotropic system ($\kappa_i = 2$ in Fan and Chen [24]). We solve Eq. (3) in a 400×400 square domain using the finite element method. To discretize the domain for all systems, a uniform mesh consisting of 22,000 triangular elements with quadratic interpolation functions is used. Time step size of iterations is $\Delta t = 0.2$. To simulate the polycrystalline material properly, 36 order parameters are used [24]. For all simulations, the initial grains configuration is similarly chosen to be a Voronoi tessellation diagram with 36 random initial orientation angles corresponding to order parameters (Fig. 4a). For cases including particles, particles are randomly distributed in the grains system where V_f and r_p are the volume fraction and size of particles, respectively.

Six different types of systems are considered:

- Type I: grains system without particles considering isotropic grain boundary energy.
- Type II: grains system without particles considering RS model.
- Type III: grains system without particles considering MRS.
- Type IV: grains system with particles considering isotropic grain boundary energy.
- Type V: grains system with particles considering RS model.
- Type VI: grains system with particles considering MRS model.

Examples of these six types of systems are presented in Fig. 4b–h. Fig. 4 reveals that including the effects of anisotropic grain boundary energy significantly alters the microstructures in both systems with and without particles.

Fig. 5 shows the average grain radius versus time of evolution in systems without particles. All systems reach a steady state grain growth rate, and this rate decreases from isotropic to anisotropic grain boundary energy models. To compare grain growth coarsening rates for systems without particles, we use the coarsening power law:

$$(r_t)^m - (r_0)^m = Kt, \tag{8}$$

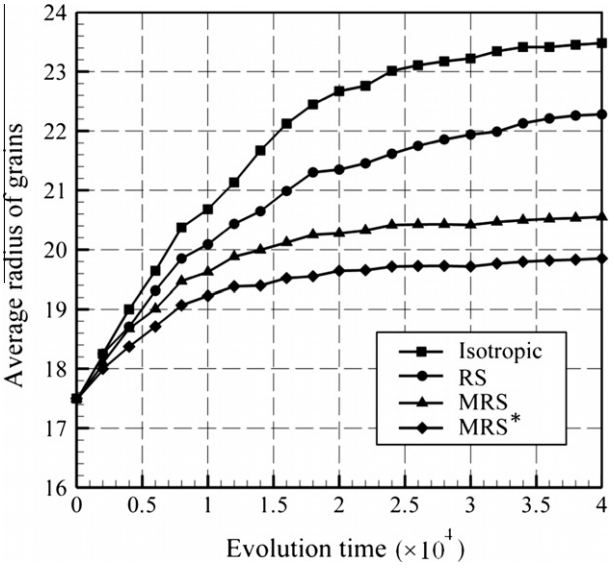

Fig. 6. Average grain radius versus time of evolution for systems with particles: $r_p = 2$, $V_f = 0.015$; $*V_f = 0.03$.

r_t and r_0 are the average radius of grains at time t and 0, respectively, K is the coarsening rate constant and is a function of volume fraction of precipitates, and m is the coarsening exponent. From Fig. 4a $r_0 \cong 17.5$. For non-linear fits in Fig. 5, the least squares method is used. The correlated values of m for isotropic, RS, and MRS are 2.06, 2.15, and 2.27, respectively.

In the cases with particles, the grain growth stops after several time steps and does not follow the coarsening power law (see Fig. 6). The previous analytical and numerical models for Zener pinning predicted a similar effect [29,32]. Accordingly, they proposed a model in which the grain growth stopped after reaching a critical average grain size ($\bar{r}_g^c$) computed to be:

$$\bar{r}_g^c = \beta \frac{r_p}{(V_f)^n}. \tag{9}$$

Values of β and n vary in different works [29,33,34]. To find these values for our model, we use $r_p = 1.5$, 2, and 2.5, and $V_f = 0.005$,

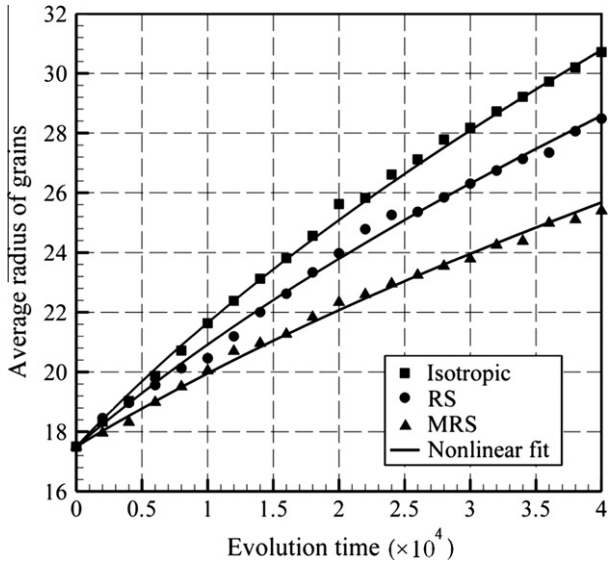

Fig. 5. Average grain radius versus time of evolution for systems without particles; nonlinear fits are plotted using Eq. (8).

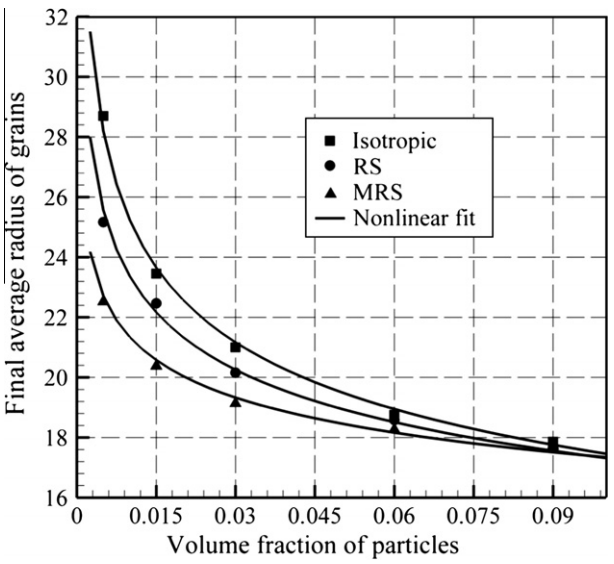

Fig. 7. Final grain size versus volume fraction of particles with $r_p = 2$; nonlinear fits are plotted using Eq. (9).

Table 1
Estimated values of β and n in (9); $0.005 \leqslant V_f \leqslant 0.09$.

	Isotropic			RS			MRS		
r_p	1.5	2	2.5	1.5	2	2.5	1.5	2	2.5
β	8.38	6.04	4.49	9.01	6.42	4.84	9.85	7.05	5.08
n	0.142	0.161	0.187	0.110	0.133	0.155	0.072	0.089	0.130

0.015, 0.03, 0.06 and 0.09. The final grain size of systems including particles with $r_p = 2$ is shown for isotropic, RS, and MRS models in Fig. 7. Estimated values for β and n are determined by fitting Eq. (9) using the least squares method (see Table 1), and these values are somehow different from those reported in previous investigations [29,33–35]. Because of their numerical algorithm, all the previous works had to consider very small initial average grain sizes, which were close to zero [29,33–35]. In reality, relatively larger grains already exist from primary recrystallization, whether static or dynamic, before or after second-phase particles nucleate and stabilize. So when higher volume fractions of particles are present in the system, i.e. grain growth is considerably slow (or no grain growth happens), the minimum average grain size is almost equal to the initial average grain size of the grain microstructure. From Fig. 6 and Table 1, it is clear that including anisotropic grain boundary energy significantly affects the grain growth morphology. The critical average grain size to stop the grain growth depends not only on volume fraction and size of particles, as predicted by other models, but also on the grain boundary energy anisotropy.

4. Conclusions

A phase-field model was used to study the concurrent effects of anisotropic grain boundary energy and presence of second-phase inert particles on grain growth rate. The concluding remarks are the following:

- Including the anisotropic grain boundary energy mitigated the grain growth, and this decrease was more significant when the effects of high misorientation angles were considered. Eventually, all systems without particles reached a steady state grain growth rate.
- The presence of particles significantly decreased grain growth rate and changed the ultimate grain microstructure. The critical average grain radius necessary to stop the grain growth was not only a function of the volume fraction and size of the second-phase particles but also significantly depended on the grain boundary energy anisotropy, especially in systems with low volume fraction of particles.

Acknowledgment

The authors would like to thank the Center for Advanced Vehicular Systems (CAVS) at Mississippi State University for supporting us on this work.

References

[1] H.K.D.H. Bhadeshia, R. Honeycombe, Steels: Microstructure and Properties, Third ed., Elsevier Ltd., 2006.
[2] K.S. Kumar, H. Van Swygenhoven, S. Suresh, Acta Mater. 51 (2003) 5743–5774.
[3] Y.B. Zhang, A. Godfrey, Q. Liu, W. Liu, D. Juul Jensen, Acta Mater. 57 (2009) 2631–2639.
[4] M.A. Azeem, A. Tewari, U. Ramamurty, Mater. Sci. Eng., A 527 (2010) 898–903.
[5] N. Goukon, T. Ikeda, M. Kajihara, Acta Mater. 48 (2000) 2959–2968.
[6] G.D. Hibbard, V. Radmilovic, K.T. Aust, U. Erb, Mater. Sci. Eng., A 494 (2008) 232–238.
[7] R.J. Contieri, M. Zanotello, R. Caram, Mater. Sci. Eng., A 527 (2010) 3994–4000.
[8] M. Kurban, U. Erb, K.T. Aust, Scripta Mater. 54 (2006) 1053–1058.
[9] H. El Kadiri, Y. Bienvenu, K. Solanki, M.F. Horstemeyer, P.T. Wang, Mater. Sci. Eng., A 421 (2006) 168–181.
[10] H. El Kadiri, L. Wang, M.F. Horstemeyer, R.S. Yassar, J.T. Berry, S. Felicelli, P.T. Wang, Mater. Sci. Eng., A 494 (2008) 10–20.
[11] R. Carel, C.V. Thompson, H.J. Frost, Acta Mater. 44 (1996) 2479–2494.
[12] W. Fayad, C.V. Thompson, H.J. Frost, Scripta Mater. 40 (1999) 1199–1204.
[13] H.J. Frost, C.V. Thompson, Curr. Opin. Solid State Mater. Sci. 1 (1996) 361–368.
[14] H.J. Frost et al., Scr. Metall. 22 (1988) (1988) 65–70.
[15] H.J. Frost, C.V. Thompson, D.T. Walton, Acta Metall. Mater. 38 (1990) 1455–1462.
[16] H.J. Frost, C.V. Thompson, D.T. Walton, Acta Metall. Mater. 40 (1992) 779–793.
[17] S.P. Riege, C.V. Thompson, H.J. Frost, Acta Mater. 47 (1999) 1879–1887.
[18] C.V. Thompson, H.J. Frost, F. Spaepen, Acta Metall. 35 (1987) 887–890.
[19] Q. Yu, S.K. Esche, Mater. Lett. 57 (2003) 4622–4626.
[20] O.M. Ivasishin, S.V. Shevchenko, N.L. Vasiliev, S.L. Semiatin, Mater. Sci. Eng., A 433 (2006) 216–232.
[21] B. Radhakrichnan, G.B. Sarma, T. Zacharia, Acta Mater. 46 (1998) 4415–4433.
[22] S. Raghavan, S.S. Sahay, Comput. Mater. Sci. 46 (2009) 92–99.
[23] G. Kugler, R. Turk, Comput. Mater. Sci. 37 (2006) 284–291.
[24] D. Fan, L.-Q. Chen, Acta Mater. 45 (1997) 611–622.
[25] M. Wang, B.Y. Zong, G. Wang, Comput. Mater. Sci. 45 (2009) 217–222.
[26] M. Wang, B.Y. Zong, G. Wang, J. Mater. Sci. Technol. 24 (2008) 829–834.
[27] A. Mallick, S. Vedantam, Comput. Mater. Sci. 46 (2009) 21–25.
[28] Y. Suwa, Y. Saito, H. Onodera, Comput. Mater. Sci. 44 (2008) 286–295.
[29] Y.-q. Long, P. Liu, Y. Liu, W.-m. Zhang, J.-s. Pan, Mater. Lett. 62 (2008) 3039–3042.
[30] S.A. Locker, F.W. Noble, J. Mater. Sci. 29 (1994) 218–226.
[31] H.P. Longworth, C.V. Thompson, J. Appl. Phys. 69 (1991) 3929–3940.
[32] F.J. Humphreys, M.G. Ardakani, Acta Mater. 44 (1996) 2717–2727.
[33] N. Moelans, B. Blanpain, P. Wollants, Acta Mater. 53 (2005) 1771–1781.
[34] N. Moelans, B. Blanpain, P. Wollants, Acta Mater. 54 (2006) 1175–1184.
[35] K. Chang, W. Feng, L.Q. Chen, Acta Mater. 57 (2009) 5229–5236.
[36] W.T. Read, W. Shockley, Phys. Rev. 78 (1950) 275–289.
[37] A. Kazaryan, Y. Wang, S.A. Dregia, B.R. Patton, Phys. Rev. B 63 (2001) 184102.
[38] M. Asle Zaeem, S.Dj. Mesarovic, J. Comput. Phys. 229 (2010) 9135–9149.
[39] M. Asle Zaeem, S.Dj. Mesarovic, Comput. Mater. Sci. 50 (2011) 1030–1036.
[40] M. Asle Zaeem, S.Dj. Mesarovic, Solid State Phenom. 150 (2009) 29–41.
[41] K. Binder, Phys. Rev. B 8 (1973) 3423–3438.
[42] J.W. Cahn, J.E. Hilliard, J. Chem. Phys. 28 (1958) 258–267.
[43] D. Wolf, Scr. Metall. 23 (1989) 1713–1718.
[44] D. Moldovan, D. Wolf, S.R. Phillpot, Philos. Mag. 83 (2003) 3643–3659.